CODAR MEASUREMENTS OF OCEAN SURFACE PARAMETERS AT ARSLOE - PRELIMINARY RESULTS

Belinda Lipa and Donald Barrick*
CODAR Research, 165 Harcross Road, Woodside, California 94062
*Wave Propagation Lab/ERL NOAA, Boulder, Colorado 80303

Abstract

We here report on a preliminary analysis of data taken by a coastal HF radar system (CODAR) which was operated during the ARSLOE experiment. The system produces the first five Fourier coefficients of the directional ocean waveheight spectrum and two-dimensional maps of radial surface current velocity. We compare our results for ocean waves with measurements made by the NDBO data buoy XERB.

1. Introduction

Over the past five years, we have been developing a compact transportable HF radar system (CODAR) for the measurement of ocean surface waves and currents. We here present results of a preliminary analysis of data taken during the ARSLOE experiment at Duck, North Carolina, in October, 1980. The basic parameters measured by CODAR are the first five angular Fourier coefficients of the ocean waveheight directional spectrum and two-dimensional maps of the surface current velocity. In the present analysis, the spatial resolutions of the resulting wave spectrum and current velocity measurements are 13 km and 2.4 km respectively. The frequency resolution is a function of ocean wave period: 0.02 Hz at 10 sec. period, 0.04 Hz at 7 sec., 0.1 Hz at 4 sec. In our final analysis we expect to achieve a spatial and frequency resolution of 5 km and 0.01 Hz in the ocean wave spectral measurements. We will also include the effects of shallow water refraction, which are ignored in this analysis.

In Section 2, we briefly describe the principles behind the operation of CODAR, showing how interpretation of the radar return in terms of electromagnetic theory leads to estimates of the ocean wave spectrum. In Section 3, we describe measurements of the ocean wave spectrum made at ARSLOE, and compare these to concurrent measurements made by the NDBO data buoy XERB, which were supplied by Dr. K. E. Steele. In Section 4, we show how to obtain the radial current velocities from the radar spectrum, and give examples of current maps made during the period of the ARSLOE storm.

2. Principles of CODAR Analysis

As with any HF radar system, interpretation of the radar spectrum to give ocean surface parameters is based on Barrick's equations (1972 a,b) for the narrow-beam radar cross section in terms of the directional ocean wave spectrum. These equations have been verified by Lipa et. al. (1981) as correctly describing the observed form of the Doppler spectrum of radar sea echo. In the absence of ocean surface currents, this consists of two dominant first-order peaks at the Bragg frequencies $\pm\omega_B$ surrounded by a continuum due to second order scatter; ω_B is given by

$$\omega_B = \sqrt{2gk_0} \qquad (1)$$

where k_0 is the radar wavenumber and g is the gravitational acceleration.

The receiving antenna of the CODAR system consists of two crossed loops and a monopole (Barrick and Lipa 1979). Signals from these antennae are combined in the software to effect the azimuthal rotation of a broad beam pattern (shaped like $\cos^4(\phi/2)$). This is illustrated schematically in Figure 1.

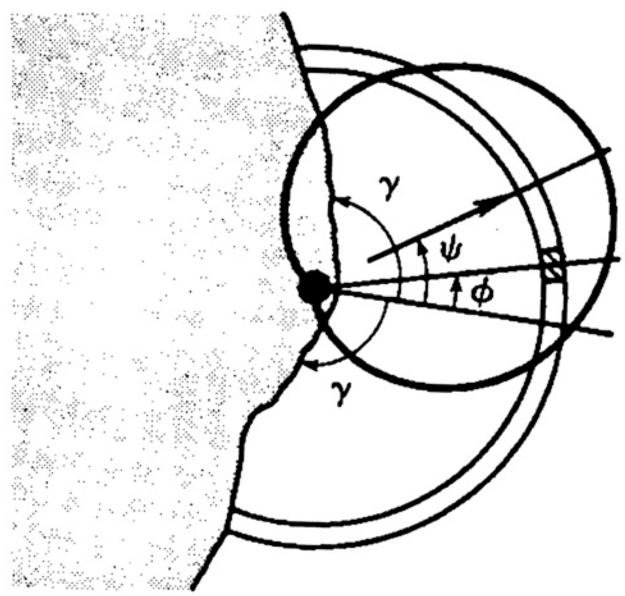

Sketch of Beam Pattern. ψ is the Scan Angle Measured from the Perpendicular to the Coast. Angles φ and γ Define the Beam Pattern and the Coastline, Respectively

Figure 1

0197-7385/82/0000-0901 $00.75

The radar return at scan angle ψ and Doppler shift ω is given by the convolution of the antenna beam pattern and the narrow-beam radar cross section:

$$\tilde{\sigma}(\omega,\psi) = \frac{1}{2\gamma} \int_{-\gamma}^{\gamma} \cos^4\left(\frac{\psi-\phi}{2}\right) \underset{\sim}{\sigma}(\omega,\phi)\, d\phi \qquad (2)$$

As shown by Barrick and Lipa (1979) equation (2) can be expressed as an angular Fourier series with five non-zero coefficients:

$$\tilde{\sigma}(\omega,\psi) = \frac{1}{2\pi} \sum_{n=-2}^{2} b_n(\omega)\, tf_n(\psi) \qquad (3)$$

where trigonometric functions are defined by

$$tf_n(\alpha) = \begin{cases} \cos(n\alpha) & \text{for } n \geq 0 \\ \sin(n\alpha) & \text{for } n < 0 \end{cases} \qquad (4)$$

The coefficients $b_n(\omega)$ can be obtained from the broad-beam radar return and are related to the narrow-beam radar cross section by the following equation:

$$b_n(\omega) = \frac{a_n \pi}{\gamma} \int_{-\gamma}^{\gamma} \underset{\sim}{\sigma}(\omega,\phi)\, tf_n(\phi)\, d\phi \qquad (5)$$

where $a_{-2} = a_2 = 1/8$; $a_{-1} = a_1 = 1/2$; $a_0 = 3/8$

Barrick's equations give $\underset{\sim}{\sigma}(\omega,\phi)$ in terms of the directional ocean waveheight spectrum, which we express as a Fourier series over angle with coefficients which are functions of the ocean wavenumber k :

$$S(k,\phi) = \sum_{n=-2}^{2} c_n(k)\, tf_n(\phi) \qquad (6)$$

Estimates of the five Fourier coefficients $c_n(k)$ are then obtained by inverting the integral equation (5). Thus CODAR produces essentially the same ocean wave information as a pitch-and-roll wave buoy.

3. ARSLOE Measurements of Ocean Wave Parameters

During the ARSLOE experiment, CODAR was located approximately 5 km north of the pier. The coastline was essentially straight, at an angle of 20° from the north-south line. Data was taken from 15 range cells, each 2.4 km in extent. In the present analysis, we have averaged the data from ranges 13 km to 26 km, assuming that the directional spectrum is homogeneous throughout this sector. We have ignored the effects of wave refraction in shallow water. The water depth in the region producing the dominant radar scatter was approximately 25 m; it follows that results can be expected to show some error for waves of period greater than 10 sec., since these waves are undergoing refraction at this depth.

The radar spectrum was inverted as described in the previous section to give the first five Fourier coefficients of the ocean wave spectrum. The zero order coefficient is the ocean wave spatial spectrum from which the temporal spectrum may be obtained. The remaining coefficients define a directional distribution at each ocean wave frequency. Examples of temporal spectra and dominant wave directions are given in Figures 2 and 3 for six time periods spanning the ARSLOE storm.

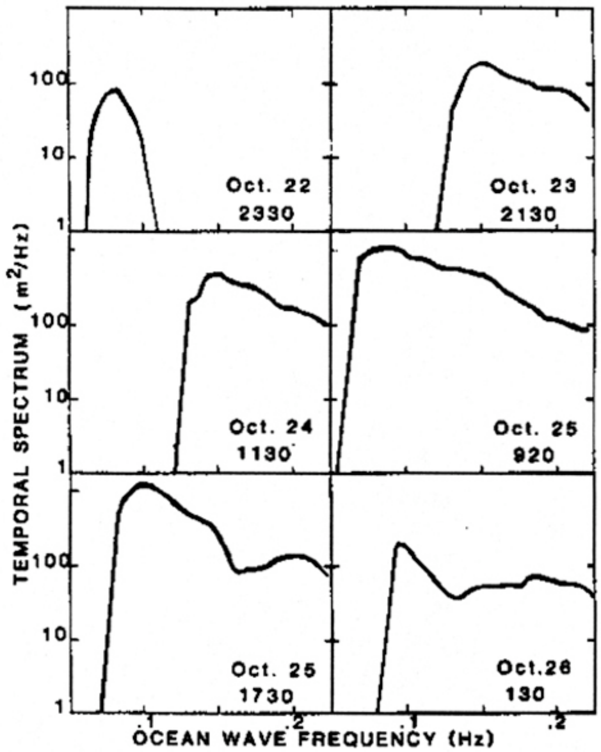

CODAR Measurements of the Ocean Wave Temporal Spectra

Figure 2

Before the start of the storm, the ocean wavefield consisted of a long period, low amplitude, onshore swell component. Storm winds started to blow onshore on the morning of October 23, continuing until around 1200 Z on October 25, when they reversed in direction, leading to the offshore short-period waves indicated in Figure 3.

Ocean wave parameters have been compared with concurrent measurements made by the pitch-and-roll wave buoy XERB, which was located about 37 km from the pier. Approximately one-half the CODAR data taken during the storm has been analyzed to date. The comparison between significant waveheight measurements is shown in Figure 4.

The two measurements agree well when the significant waveheight is less than 3.5 m. At higher waveheights, the radar spectrum saturates and the perturbation theory on which the radar analysis is based breaks down, leading to waveheight estimates that are too low. The radar saturation region is defined approximately by the

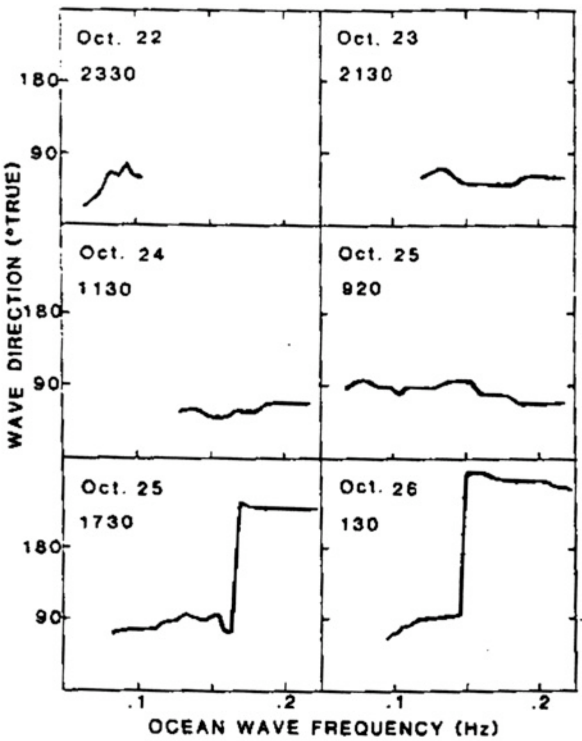

CODAR Measurements of the Dominant Wave Direction

Figure 3

inequality $k_o h > 0.5$ where k_o is the radar wavenumber and h is the rms waveheight. This limit is shown by the dashed line in Figure 4 for the CODAR transmit frequency of 25.4 MHz. A simple way to avoid this problem is to lower the radar transmit frequency when saturation occurs; in all future CODAR measurements we will operate at 5 MHz when the waveheight exceeds 3.5 m.

The comparison between the peak periods of measured ocean wave spectra is shown in Figure 5. The periods of the short-period waves (< 10 sec.) agree to within a second; long-period waves ($\geq$ 10 sec.) to within 2 sec.

The comparison between wave directions is shown in Figure 6. For both CODAR and XERB, we define a mean wave direction using the ratio of the first-order coefficients:

$$\phi = \tan^{-1} (c_{-1}/c_1) \tag{7}$$

The directions agree to within a few degrees for short wave periods; the agreement is less good for longer period waves, because we have not yet allowed for their refraction into shallow water.

Table 1 gives the bias of CODAR wave parameters relative to those measured by XERB, based on the 14 CODAR events in the storm period outside the radar saturation region. Sampling times were 36 min for the radar and 17 min for the buoy. Long/short waves are defined as having periods greater/less than 10 sec. We have calculated the bias in short wave direction for two periods: 1200Z, October 23 to 1200Z, October 24 when the wind direction was stable and the period after

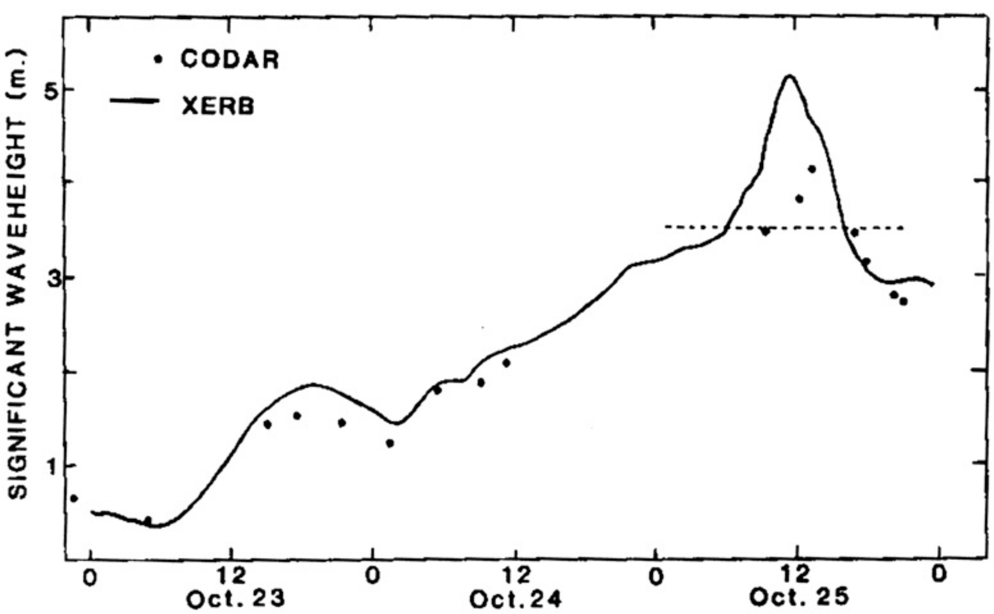

Waveheight Comparison. The Dashed Line Indicates the Radar Saturation Level

Figure 4

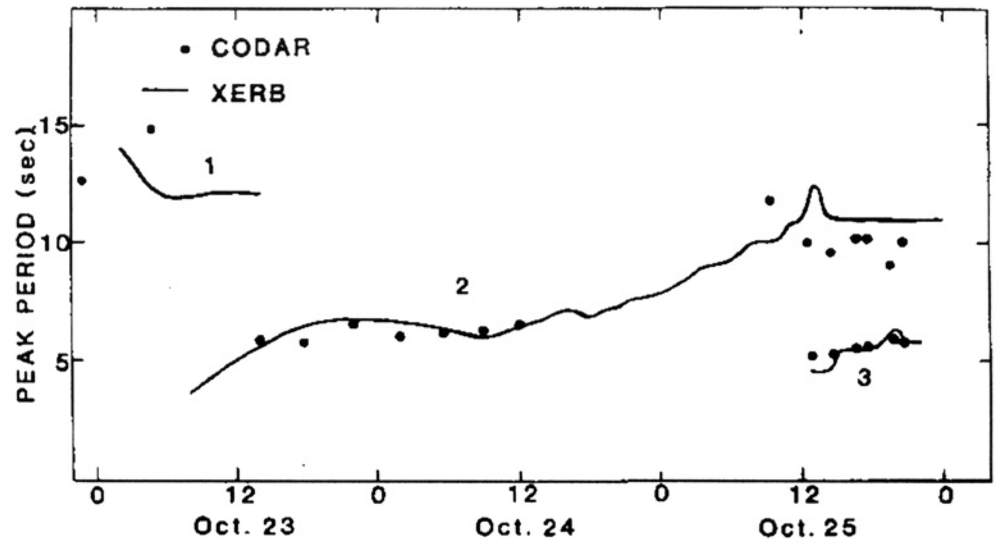

Comparison between Ocean Wave Peak Periods. Three Wave Trains are Indicated - 1: Long Period Swell. 2: Onshore Storm Waves. 3: Offshore Storm Waves

Figure 5

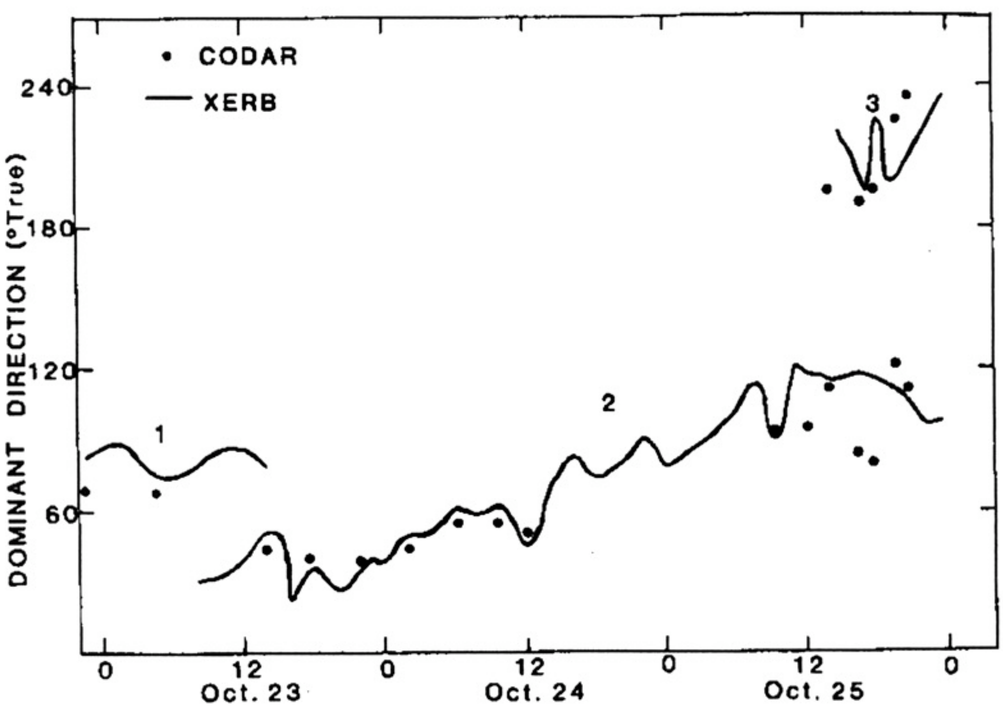

Wave Direction Comparison. Wave Trains are Numbered as in Figure 5

Figure 6

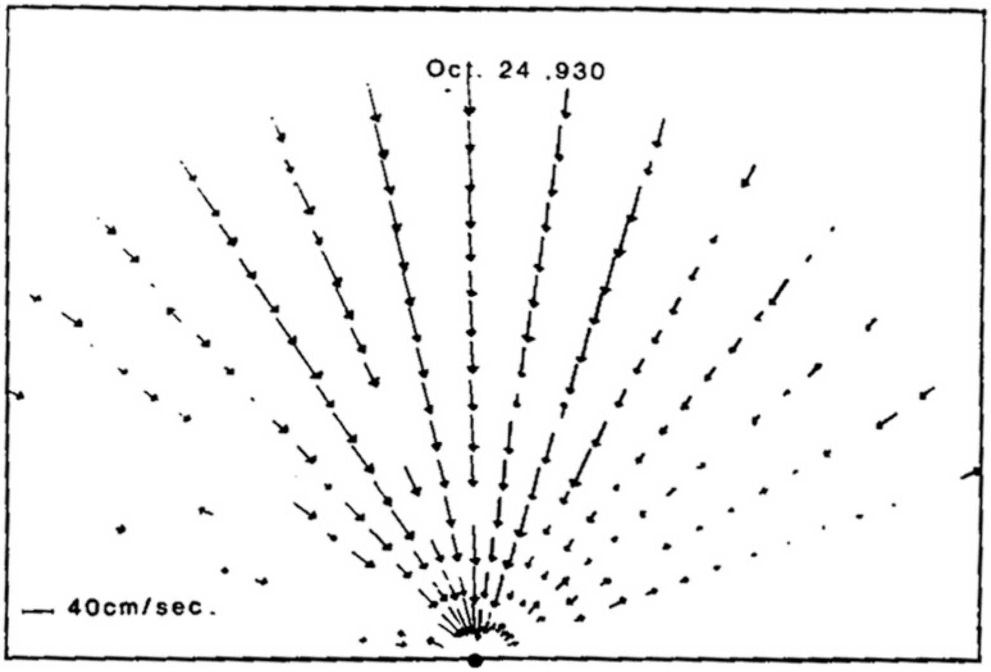

Radial Surface Current Velocity Pattern Observed with Onshore Storm Winds. The Length of the Arrows is Proportional to the Current Speed; the Length Corresponding to 40 cm/sec is Shown on the Left

Figure 7

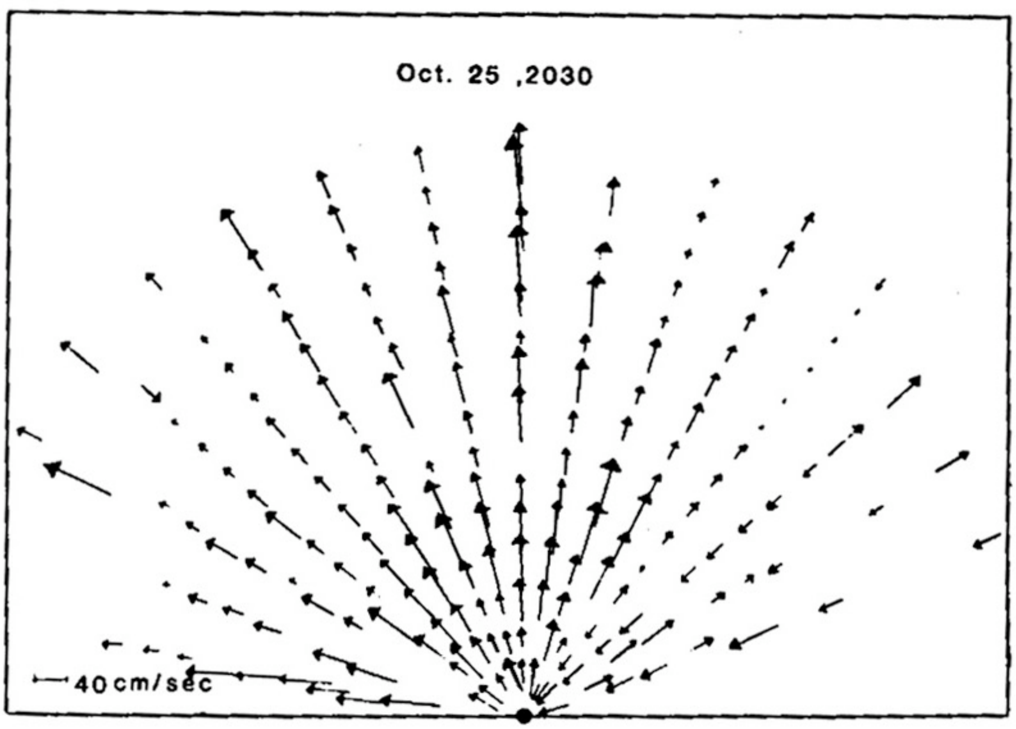

Radial Surface Current Velocity Pattern Observed with Offshore Storm Winds

Figure 8

1200Z, October 25, when the wind was veering rapidly. Larger bias should be expected during the latter period because of the different locations of the two instruments.

Table I: Comparison between CODAR and XERB

	Mean Bias	Maximum Bias
Significant waveheight	-.12m (-5.5%)	-0.5m
Long wave period	-0.5 sec	-2 sec
Short wave period	0.1 sec	0.9 sec
Long wave direction	-15^o	-36^o
Short wave direction (stable wind direction)	0.04^o	-9^o
Short wave direction (rapidly veering wind)	2.4^o	$\pm 33^o$

4. Surface Current Measurements

In the presence of ocean surface currents, equation (5) becomes

$$b_n(\omega) = \frac{a_n \pi}{\gamma} \int_{-\gamma}^{\gamma} \underset{\sim}{\sigma}(\omega - 2k_o v_R(\phi), \phi) tf_n(\phi) d\phi \qquad (8)$$

where $v_R(\phi)$ is the radial current velocity at angle ϕ. The first order narrow-beam radar cross section is an impulse function at the Bragg frequencies defined by (1):

$$\sigma^{\pm}(\omega, \phi) = \delta(\omega \mp \omega_B) \quad \mu^{\pm}(\phi) \qquad (9)$$

where $\mu^{\pm}(\phi)$ is the first-order sea echo for the advancing/receding Bragg waves. Substituting (9) into (8) gives for the first-order region:

$$b_n^{\pm}(\omega) = \frac{a_n \pi}{\gamma} \int_{-\gamma}^{\gamma} \delta(\omega \mp \omega_B - 2k_o v_R(\phi)) \mu^{\pm}(\phi) \; tf_n(\phi) d\phi \qquad (10)$$

It follows from (10) that in the presence of ocean currents, the first-order "line" is spread out in frequency. We can derive the radial current velocity pattern by interpretation of the first-order structure. Assuming that a given value of velocity occurs at most at two angles ϕ_1 and ϕ_2, equation (10) can be written

$$b_n^{\pm}(2k_o v_R) = K_1^{\pm}(\phi_1) tf_n(\phi_1) + K_2^{\pm}(\phi_2) tf_n(\phi_2) \qquad (11)$$

where

$$K_i^{\pm}(\phi) = \frac{a_n \pi}{\gamma} \quad \mu^{\pm}(\sigma_i) \qquad (12)$$

The set of equations (11) can be solved in the least-squares sense at each value of Doppler frequency to give ϕ_1 and ϕ_2 as a function of the current velocity v_R. Inversion of the derived relationship gives the current velocity pattern, $v_R(\phi)$.

Figures 7 and 8 show the radial current velocity pattern measured before and after the wind wave reversal occurring at 1200Z October 25. We have found that the direction of the maximum current followed the wind direction with a time lag of about 8 hours and that the current speed was about 2.7% of the wind speed.

5. Conclusion

Our preliminary analysis indicates that CODAR was operated successfully during the ARSLOE experiment to produce measurements of ocean waves and currents. We expect the accuracy and resolution of these results to increase with improved analysis techniques.

References

Barrick, D. E. (1972a): "First order theory and analysis of MF/HF/VHF scatter from the sea", IEEE Trans. Antennas Propagat., AP-20, 2-10.

Barrick, D. E. (1972b): "Remote sensing of sea-state by radar", Remote Sensing of Troposphere, ed. V. E. Derr, U.S. Government Printing Office, Washington, D.C.

Barrick, D. E. and B. J. Lipa (1981): "A compact transportable HF radar system for directional coastal wavefield measurements", in Ocean Wave Climate, ed. M. D. Earle and A. Malahoff (Plenum, New York) 153-201.

Lipa, B. J., D. E. Barrick and J. W. Maresca, Jr. (1981): "HF radar measurements of long ocean waves", J. Geophys. Res., 86, 4089-4102.